

where

$$G_2 = (5,225,472 + 7,983,360\beta + 4,717,440\beta^2 + 1,340,640\beta^3 + 181,272\beta^4 + 9158\beta^5)a_0 + (2,115,072 + 3,265,920\beta + 1,982,880\beta^2 + 584,640\beta^3 + 82,560\beta^4 + 4375\beta^5)a_1 \quad (38)$$

Note that  $G_2 = 0$  has only negative roots. It is always positive for physically realizable values of  $\beta$ , namely,  $\beta > 0$ . Figure 3 shows the dependence of the stiffness vs  $\xi$  for different values of the elastic coefficient  $\beta$ . The natural frequency squared reads

$$\begin{aligned} \omega^2 &= 504b_5/a_1 \\ &= 2,580,480(3 + \beta)^5 b_0 / G_2 \end{aligned} \quad (39)$$

Because  $G_2$  is positive, so is the natural frequency for  $\beta > 0$ .

When the elastic coefficient vanishes, the stiffness and the natural frequency read, respectively,

$$\begin{aligned} D(\xi) &= b_0 + [12(435,456a_0 + 176,256a_1)\xi + 144(-24,192a_0 \\ &+ 14,688a_1)\xi^2 - 1728(2016a_0 + 1296a_1)\xi^3 + 20,736(84a_0 \\ &- 108a_1)\xi^4 + 1,244,160a_1\xi^5]b_0 / (5,225,472a_0 + 2,115,072a_1) \\ \omega^2 &= 627,056,640b_0 / (5,225,472a_0 + 2,115,072a_1) \end{aligned} \quad (40)$$

When the elastic coefficient tends to the infinity, the stiffness and the natural frequency tend to the following respective expressions:

$$\begin{aligned} D(\xi) &= b_0 + [4(1960a_0 + 1047a_1)\xi + 16(168a_0 + 215a_1)\xi^2 \\ &- 64(280a_0 - 7a_1)\xi^3 + 256(28a_0 - 45a_1)\xi^4 \\ &+ 5120a_1\xi^5]b_0 / (9128a_0 + 4375a_1) \\ \omega^2 &= 2,580,480b_0 / (9128a_0 + 4375a_1) \end{aligned} \quad (41)$$

Figure 3 shows the variation of the stiffness for various values of  $\beta$ .

In an analogous manner one can determine the closed-form solutions for natural frequencies of beams with parabolic, cubic, quartic, etc., variations of the mass density.

### Summary

This study presents a simple closed-form solution for the natural frequency and the mode shape of the inhomogeneous beam with rotational spring. The author is unaware of any other closed-form solution for the homogeneous or inhomogeneous beam with a spring. Analogous treatment can be performed for beams with springs at each end.

### Acknowledgments

The author acknowledges support from the National Science Foundation, Program Director K. P. Chong, through Grant 99-10195. Help in numerical calculations from Roland Becquet of the Laboratoire de Recherches et Applications en Mécanique Avancée, France, is gratefully acknowledged.

### Reference

- <sup>1</sup>Candan, S., and Elishakoff, I., "Infinite Number of Closed-Form Solutions for Reliability of Structures," *Applications of Statistics and Probability*, edited by R. E. Melchers and M. G. Stewart, Balkema, Rotterdam, The Netherlands, 2000, pp. 1059-1068.

A. Berman  
Associate Editor

## Prediction of Fundamental Frequencies of Stressed Spring-Hinged Tapered Beams

G. Venkateswara Rao\* and N. Rajasekhara Naidu†  
Vikram Sarabhai Space Center,  
Trivandrum 695 022, India

### Introduction

INTERSTAGES, thrust frames, payload adapters, etc., of rocket/missile structural systems are often configured with beams attached to end rings. The beams are joined to the end rings, and based on the joint configuration the ends of the beams are usually idealized using end rotational constraints, the stiffness parameter value of which is fixed based on the quality of the joint. These beams during their service conditions are subjected to compressive loads. Further, the vibration behavior of these beams, especially the fundamental frequency of prediction, is most important for evaluation of the transmissibility of gravitational acceleration loads due to the flight dynamic environment. To save mass, these beams are often designed as tapered beams, which are near optimum for engineering purposes.

Quick prediction and information about the fundamental frequency of such beams under initial stress is of significant importance during their design phase. The finite element method is widely used to estimate the fundamental frequency of beams with initial stresses.<sup>1-5</sup> End rotational constraints are considered in Refs. 6-10. Though the finite element method is versatile, closed-form solution is very elegant and yields quick results. In this Note, a simple formula is derived to predict the fundamental frequency of stressed tapered beams with end rotational restraints when its stress free frequency is known. It is assumed that the mode shapes for the buckling and free vibration are the same as that of the initially stressed vibration of the tapered beam. A set of numerical results for tapered beams with end rotational restraints having symmetric linear variation in depth and constant breadth are generated for various values of rotational stiffness parameters using the formula. The finite element method (the beam is idealized using 20 tapered elements) is employed to verify these results. The details of the formulation and the numerical results are presented.

### Formulation

Consider a beam of length  $L$ , moment of inertia  $I(x)$ , where  $x$  is the axial coordinate,  $E$  Young's modulus, and  $\rho$  mass density with an end concentrated load  $P$  (Fig. 1). If the beam is executing harmonic oscillations, then the governing matrix equation of the free vibrations of the initially stressed beam is given by the standard equation

$$[K]\{\delta\} - \lambda[G]\{\delta\} - \lambda_f[M]\{\delta\} = 0 \quad (1)$$

where  $[K]$ ,  $[G]$ , and  $[M]$  are the assembled elastic stiffness matrix with the proper contribution of end rotational spring stiffness, geometric stiffness matrix, and mass matrix, respectively, and  $\lambda$  is the axial compressive load parameter, which is time invariant (defined as  $\lambda = PL^2/EI_0$ , where  $I_0$  is the reference moment of inertia at the ends of the beam), and  $\lambda_f$  is the frequency parameter (defined as  $\lambda_f = \rho A_0 \omega^2 L^4 / EI_0$ , where  $\omega$  is the circular frequency,  $A_0$  is the reference cross-sectional area at the ends of the beam), and  $\{\delta\}$  is the eigenvector.

From Eq. (1), the degenerate case of the stability equation is given by

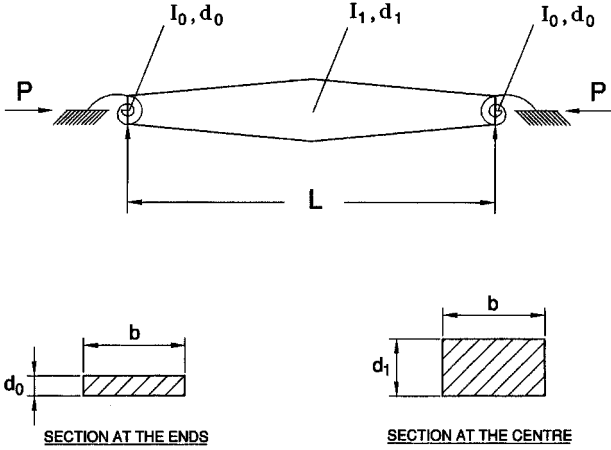
Received 25 March 2000; revision received 24 August 2000; accepted for publication 31 August 2000. Copyright © 2000 by the American Institute of Aeronautics and Astronautics, Inc. All rights reserved.

\*Group Director, Structural Engineering Group.

†Scientist/Engineer, Structural Engineering Group.

**Table 1** Fundamental frequency parameter  $\lambda_f$  of tapered beams for  $\alpha = 1.0$ 

Depth	0.0	0.2	0.4	0.6	0.8	1.0	$\lambda_b$
$\bar{d} = 1.0$							13.49
FEM	133.4	106.8	80.23	53.60	26.97	0.0	
Eq. (6)	133.4	106.8	80.07	53.38	26.69	0.0	
% Difference with FEM	0.0	0.0	-0.1994	-0.4104	-1.038	—	
$\bar{d} = 1.1$							15.88
FEM	146.5	117.3	88.12	58.95	29.76	0.0	
Eq. (6)	146.5	117.2	87.87	58.58	29.29	0.0	
% Difference with FEM	0.0	-0.8525	-0.2837	-0.6276	-1.579	—	
$\bar{d} = 1.3$							21.35
FEM	174.3	139.6	105.1	70.54	35.99	0.0	
Eq. (6)	174.3	139.3	104.5	69.66	34.83	0.0	
% Difference with FEM	0.0	-0.2149	-0.5709	-1.247	-3.223	—	
$\bar{d} = 1.5$							27.78
FEM	204.2	163.7	123.4	83.16	42.89	0.0	
Eq. (6)	204.2	163.1	122.3	81.56	40.78	0.0	
% Difference with FEM	0.0	-0.3665	-0.8914	-1.924	-4.920	—	

**Fig. 1** Tapered column with rotational end restraints.

$$[K]\{\delta\} = \lambda_b [G]\{\delta\} \quad (2)$$

where  $\lambda_b$  is the stability parameter (defined as  $\lambda_b = P_{cr} L^2 / E I_0$ , where  $P_{cr}$  is the critical load). Equation (2) can be written as

$$[G]\{\delta\} = (1/\lambda_b)[K]\{\delta\} \quad (3)$$

Similarly, a degenerate case for the vibration problem from Eq. (1) can be written as

$$[M]\{\delta\} = (1/\lambda_{f0})[K]\{\delta\} \quad (4)$$

where  $\lambda_{f0}$  is the frequency parameter of the beam where there is no initial stress.

Assuming that the eigenvectors for the buckling and free vibration are the same as that of the initially stressed vibration of the beam and substituting Eqs. (3) and (4) in Eq. (1), we get

$$[K]\{\delta\} - (\lambda/\lambda_b)[K]\{\delta\} - (\lambda_f/\lambda_{f0})[K]\{\delta\} = 0 \quad (5)$$

Equation (5) implies that

$$(\lambda/\lambda_b) + (\lambda_f/\lambda_{f0}) = 1 \quad (6)$$

From Eq. (6), where  $\lambda$  (axial load parameter for a particular value of  $P$ ),  $\lambda_b$ , and  $\lambda_{f0}$  are known, one can compute the frequency parameter  $\lambda_f$  of the initially stressed beam.

**Table 2** Fundamental frequency parameter  $\lambda_f$  of tapered beams for  $\alpha = 100.0$ 

Depth	0.0	0.2	0.4	0.6	0.8	1.0	$\lambda_b$
$\bar{d} = 1.0$							37.95
FEM	464.0	371.1	277.4	182.7	86.86	0.0	
Eq. (6)	464.0	371.2	278.4	185.6	92.81	0.0	
% Difference with FEM	0.0	0.02694	0.3605	1.587	6.650	—	
$\bar{d} = 1.1$							43.72
FEM	485.9	388.1	289.5	190.1	89.80	0.0	
Eq. (6)	485.9	388.7	291.5	194.4	97.18	0.0	
% Difference with FEM	0.0	0.1546	0.6908	2.262	8.218	—	
$\bar{d} = 1.3$							56.39
FEM	531.3	423.5	315.0	206.0	96.24	0.0	
Eq. (6)	531.3	425.1	318.8	212.5	106.3	0.0	
% Difference with FEM	0.0	0.3778	1.206	3.155	10.45	—	
$\bar{d} = 1.5$							70.58
FEM	578.7	460.6	342.0	222.9	103.3	0.0	
Eq. (6)	578.7	463.0	347.2	231.5	115.7	0.0	
% Difference with FEM	0.0	0.5210	1.520	3.858	12.00	—	

## Numerical Results and Discussion

By use of the present formulation, the fundamental frequency parameter  $\lambda_f$  of the initially stressed tapered beam (with end rotational constraints) of rectangular cross section with linearly varying depth taper and constant breadth, as shown in Fig. 1, has been computed. The taper ratio is defined as  $\bar{d} = d_1/d_0$ , where  $d_0$  and  $d_1$  are depths of the beam at the ends and the center, respectively. The values of  $\lambda_f$  obtained from Eq. (6) for tapered beams with end rotational constraints are tabulated for various values of initial stress parameter  $\bar{\lambda} = \lambda/\lambda_b$ , depth parameter (taper ratio)  $\bar{d}$ , and for two values of end rotational stiffness parameter  $\alpha (kL/EI_0)$ , where  $k$  is the stiffness of the rotational spring, namely,  $\alpha = 1.0$  and  $100.0$ , and are given in Tables 1 and 2. The values of  $\lambda_b$  and  $\lambda_{f0}$  are computed using the standard finite element method (FEM) using 10 tapered finite elements of equal length. This element idealization is fixed based on the convergence study and gives accurate results up to four significant figures. A two-noded tapered beam element developed as per the standard procedure<sup>11</sup> is employed for computing the finite element results. The parameter  $\lambda_f$  obtained from the FEM using Eq. (1) is also presented in Tables 1 and 2 for comparison. The percentage difference of the results obtained by Eq. (6) with respect to those

obtained by the FEM is also included in Tables 1 and 2. Noted that for the values of  $\alpha$  considered in this Note, for  $\alpha = 0.0, 0.1$ , and  $1.0$ , Eq. (6) gives an underestimate. For  $\alpha = 10.0, 100.0$ , and for  $\alpha \rightarrow \infty$ , Eq. (6) gives an overestimate for the stressed frequency. This is due to the effect of the variation of the mode shapes changing from the simply supported case to the clamped case. The results are presented in this Note for the two typical values of  $\alpha = 1.0$  and  $100.0$  only. It can be seen from Tables 1 and 2 that the present results are in good agreement with the finite element results with the initial stress parameter  $\bar{\lambda}$  up to  $0.6$ ; the error is less than  $3.5\%$ . However for higher values of  $\bar{\lambda}$ , for example,  $0.8$ , the results differ by about  $5\text{--}12\%$ , depending on the values of  $\alpha$  and  $\bar{d}$ . The results for  $\alpha = 0.0$  (simply supported tapered beam),  $0.1, 10.0, 100.0$  and  $\alpha \rightarrow \infty$  (clamped tapered beam) are also computed, but not given here for the sake of brevity, and show the same trend. This is because the eigenvectors for higher values of  $\bar{\lambda}$  are not exactly the same, violating the assumption made in the present analysis. However, for all practical purposes the present results are good enough and can be used effectively and quickly by design engineers to assess the fundamental frequency parameter of initially stressed beams with end rotational restraints.

### Conclusions

A simple formula is proposed to predict the fundamental frequency of initially stressed tapered beams with end elastic rotational restraints for a given initial stress by knowing its stress free frequency. Because fundamental frequency is one of the important design parameters during the design phase of any structural element, a quick method of its estimation with minimum computational effort is very useful for designers. The proposed formula is expected to meet this requirement. Numerical results presented for typical tapered beams with end elastic rotational restraints demonstrate its applicability. These results are found to be in reasonably good agreement with those obtained from the FEM and, hence, can be effectively used during the design phase.

### References

- <sup>1</sup>Shastri, B. P., and Venkateswara Rao, G., "Initially Stressed Vibrations of Beams with Two Symmetrically Placed Intermediate Supports," *Journal of Sound and Vibration*, Vol. 103, No. 4, 1985, pp. 593–595.
- <sup>2</sup>Kanaka Raju, K., and Venkateswara Rao, G., "Free Vibration Behaviour of Prestressed Beams," *Journal of Structural Engineering*, Vol. 112, No. 2, 1986, pp. 433–437.
- <sup>3</sup>Singarvelu, J., Singh, G., and Venkateswara Rao, G., "Free Flexural Vibrations of Initially Stressed Tapered Beams Including the Effects of Shear Deformation and Rotary Inertia," *Journal of Sound and Vibration*, Vol. 158, No. 3, 1992, pp. 572–575.
- <sup>4</sup>Shastri, B. P., and Venkateswara Rao, G., "Vibrations of Partially Stressed Beams," *Journal of Vibration, Acoustics, Stress and Reliability in Design*, Vol. 108, No. 4, 1986, pp. 474–475.
- <sup>5</sup>Kanaka Raju, K., and Venkateswara Rao, G., "Vibration Behaviour of Tapered Beams Columns," *Journal of Engineering Mechanics*, Vol. 114, No. 5, 1988, pp. 889–892.
- <sup>6</sup>Lee, Y. S., and Ke, H. Y., "Free Vibrations of a Non-Uniform Beam with General Elastically Restrained Boundary Condition," *Journal of Sound and Vibration*, Vol. 136, No. 3, 1990, pp. 425–437.
- <sup>7</sup>Gutierrez, R. H., Laura, P. A. A., and Rossi, R. E., "Natural Frequencies of a Timoshenko Beam of Non-Uniform Con-Section Elastically Restrained at Core End and Guided at the Other," *Journal of Sound and Vibration*, Vol. 141, No. 1, 1990, pp. 174–189.
- <sup>8</sup>Maurizi, M. J., Bambill De Rossit, D. V., and Laura, P. V. V., "Free and Forced Vibrations of Beams Elastically Restrained Against Translation and Rotation at the Ends," *Journal of Sound and Vibration*, Vol. 120, No. 3, 1988, pp. 626–630.
- <sup>9</sup>Sato, K., "Transverse Vibrations of Linearly Tapered Beams with Ends Rotational Elastically Against Rotation Subjected to Axial Force," *International Journal of Mechanical Sciences*, Vol. 22, No. 2, 1980, pp. 109–115.
- <sup>10</sup>Venkateswara Rao, G., Rajasekhara Naidu, N., "Free Vibration and Stability Behaviour of Uniform Beams and Columns with Nonlinear Elastic End Rotational Restraints," *Journal of Sound and Vibration*, Vol. 176, No. 1, 1994, pp. 130–135.
- <sup>11</sup>Zienkiewicz, O. C., *The Finite Element Method*, McGraw-Hill, London, 1977.

A. Berman  
Associate Editor

## Visualization Study of a Passively Perturbed Swirling Jet

T. Terry Ng\*

University of Toledo, Toledo, Ohio 43606

### I. Introduction

THE effect of flow disturbances on jet development is a phenomenon of major practical significance. In addition to the instabilities governing the spanwise vortex development, the computational study by Pierrehumbert and Widnall<sup>1</sup> identifies a broadband fundamental mode instability that leads to a streamwise vorticity concentration. A number of studies in recent years have also been focused on forcing other instabilities such as the low-level azimuthal modes and on controlling the jet flow by alterations of the nozzle geometry. Two examples of these studies are Long and Petersen<sup>2</sup> and Longmire et al.<sup>3</sup>

Recent advances in actuator technology allowed an elaborate control scheme by Davis and Glezer.<sup>4</sup> In this scheme an azimuthal array of nine synthetic jet actuators was placed around the circumference of a round jet exit. The control was used to manipulate both mixing at the small scale and entrainment at the large scale. Many modes of jet flow could be induced. Additionally to jets consisting of mostly axial flow, there have also been many investigations on jets with swirl. A recent example is that of Wicker and Eaton,<sup>5</sup> where streamwise vorticity with an opposite sign to the main swirl was injected using four vortex generators placed evenly deep inside a nozzle. A four-lobed structure was subsequently observed in the jet.

In this investigation the effects of small, discrete perturbations around the perimeter of a jet with and without swirl are studied. The main objective of present effort is to establish a relationship between the number of perturbations and the resulting flow structure. The work is mostly qualitative, with flow visualization being the main tool.

### II. Experimental Setup

The experiment was conducted in a jet flow apparatus consisting of a 25-mm-diam, 60-mm-long nozzle attached to a 14-cm-diam stagnation chamber. Screens, perforated plates, and flow straighteners are positioned inside the stagnation chamber and upstream of a single 5-cm diam side entrance, which provides the swirling component.

Five different jet exit geometries, each with a nominal diameter of 2.22 cm and length of 24 mm, were tested. The baseline geometry is circular and is designated N-00. Other jet exits, shown in Fig. 1, are designated N-02, N-03, N-04, and N-08 with the numeral indicating the number of perturbations. Perturbations on the N-02, N-03, and N-08 exits are in the form of small, circular-arc notches at the exit circumference. The notches are approximately 7.0 mm in width and 1.5 mm in depth. Merging every two notches on the N-08 geometry formed the N-04 exit.

The experiment was conducted at a Reynolds number of approximately  $1.8 \times 10^4$  based on the nominal exit diameter and the main (nonswirling) flow. The exit flow characteristics were quantified using a single hot-wire probe. Results for all of the exit geometries indicate a uniform exit velocity profile with an exit boundary-layer thickness of about 1 mm and an initial turbulent level of 0.4%.

For convenience the main flow is held fixed. The ratio of side-to-main volumetric flow is about 0.25. Although the addition of side flow increases the Reynolds number, qualitatively and visually the development of the jet did not seem particularly sensitive to moderate variations in the overall flow rate. The smoke for flow visualization was generated using a Rosco fog machine, with either a strobe light or laser sheet providing the illumination. Images were

Received 3 April 2000; revision received 3 August 2000; accepted for publication 18 August 2000. Copyright © 2000 by the American Institute of Aeronautics and Astronautics, Inc. All rights reserved.

\*Professor, Department of Mechanical Engineering.